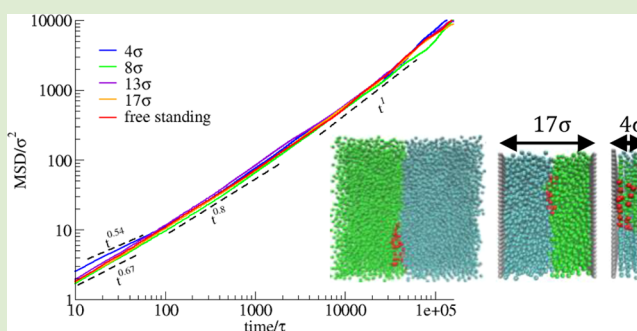


Scaling Behavior of Polymers at Liquid/Liquid Interfaces

Tseden Taddese,[†] David L. Cheung,[‡] and Paola Carbone^{*,†}[†]School of Chemical Engineering and Analytical Science, The University of Manchester, Oxford Road, Manchester M13 9PL, United Kingdom[‡]School of Chemistry, National University of Ireland Galway, Galway, Ireland

Supporting Information

ABSTRACT: The dynamics of a polymer chain confined in a soft 2D slit formed by two immiscible liquids is studied by means of molecular dynamics simulations. We show that the scaling behavior of a polymer confined between two liquids does not follow that predicted for polymers adsorbed on solid or soft surfaces such as lipid bilayers. Indeed, our results show that in the diffusive regime the polymer behaves like in bulk solution, following the Zimm model, and with the hydrodynamic interactions dominating its dynamics. Although the presence of the interface does not affect the long-time diffusion properties, it has an influence on the dynamics at short time scale, where for low molecular weight polymers the subdiffusive regime almost disappears. Simulations carried out when the liquid interface is sandwiched between two solid walls show that, when the confinement is a few times larger than the blob size, the Rouse dynamics is recovered.



Simulations carried out when the liquid interface is sandwiched between two solid walls show that, when the confinement is a few times larger than the blob size, the Rouse dynamics is recovered.

The prediction of structural and dynamical properties of polymers at liquid/liquid interfaces is both a technological and a biological problem. Indeed, polymers are confined at or pass through liquid interfaces in many industrial processes, such as liquid/liquid extractions, solvent displacement methods, or emulsifications, and also when used for biological applications, such as drug nanocarriers, biocompatibilizers, or protective coatings.^{1–3} In these situations, the polymer chains can dissolve in one of the two solvents or reside at the interface, depending on their relative solubility. The latter case is quite common since, in order to lower the interfacial free energy, polymers can be adsorbed at the interface, behaving as surface active molecules.^{4–7} When this situation occurs, the polymer chain is confined in a “soft slit” characterized by a solvent density that is lower than the bulk one. The experimental characterization of polymers entrapped at soft interfaces is very challenging, and the most common soft interface used is that formed by phospholipid bilayers. The binding of the macromolecules on the fluid surface formed by lipid molecules modifies both the macromolecule and the interface dynamics. Upon adsorption of polymer chains on supported lipid bilayers, the lipids show dynamical heterogeneity with a bimodal distribution of their diffusion coefficients at low polymer coverage.^{8,9} As expected, the dynamics of the polymer itself is also affected by the adsorption and presents an unexpected dependency with the polymer molecular weight. Maeir and Radler¹⁰ studied the dynamics of double-stranded DNA chains adsorbed on lipid membranes in fluid state. They found that the polymer radius of gyration (R_g) values follow the predicted scaling law $R_g \sim N^{-3/4}$ for a two-dimensional random walk, and the polymer self-diffusion coefficient (D) scales with the chain monomer

number (N) following the Rouse-like regime ($D \sim N^{-1}$), indicating that the hydrodynamic interactions (HI) are screened in this situation. Similar results have also been obtained by Zhang and Granick⁹ using synthetic macromolecules adsorbed on lipid monolayers. Explanations for such screening included the possibility that the lateral movements of the lipids dissipate energy, reducing the HI, and that the polymer enters a reptation-like regime when confined on an inhomogeneous surface.^{11,12}

If the experimental characterization of macromolecule dynamics at soft interfaces is difficult, their simulation is also challenging. The available literature^{11–18} focuses only on the modeling of polymer confined between solid surfaces (flat as in a slit pore or rounded as in cylindrical pores) dissolved in a good solvent often modeled as a continuum defined by a friction coefficient and therefore ignoring any HI. For example, Mukherji et al.¹⁹ performed molecular dynamics (MD) simulations of a bead-and-spring polymer model adsorbed on an attractive corrugated solid surface using implicit (good) solvent. They found that, depending on the polymer topology and the strength of the adsorption, D scales with N following two scaling laws: $D \sim N^{-3/2}$ for strongly adsorbed linear chains (reptation-like regime) and $D \sim N^{-1}$ (Rouse-like regime) for ring polymers. The Rouse-like regime was also found for solid surface with reduced roughness and for polymers adsorbed on solid substrate, where the distance between the surface defects equals the monomer bond length. Desai et al. used both

Received: July 7, 2015

Accepted: September 9, 2015

Published: September 14, 2015

implicit¹⁴ and explicit solvent¹¹ MD simulations to model a single polymer chain confined in two dimensions. The implicit solvent simulations, on a surface containing impenetrable obstacles, predicted a cross over between Rouse-type and reptation-like behavior when the spacing between the obstacles became comparable to the polymer end-to-end distance. Using explicit solvent, the same authors recovered the Rouse-like behavior ($D \sim N^{-1}$) for no-slip or corrugated surfaces, but predicted a different scaling law, $D \sim N^{-3/4}$, for a polymer adsorbed on an ideal smooth surface.

Although these simulations clarified that the roughness of the solid surface plays an important role in determining the dependence of D with the chain length, they did not answer the question of what happens when the polymer chain is adsorbed on a soft penetrable surface. Using an analytical approach, Ramachandran et al.²⁰ derived the mobility tensor for a Gaussian polymer chain embedded in a liquid membrane surrounded by bulk solvent and walls. The authors found that a crossover between the Rouse and the Zimm-like dynamics is indeed observed when the membrane is respectively sandwiched between two walls or left unconstrained, and we will show later that our molecular simulations agree with the theory and show the same change in behavior when a liquid interface is confined between two walls in close proximity. Here we perform MD simulations where one single polymer chain is confined in a 2D soft slit formed by two immiscible liquids, both modeled as good solvent. The polymer chain and the solvents are modeled using the same Lennard-Jones model we employed in our previous work.^{4,5} Since the surface tension between the two liquids is high enough and the polymer conformational entropy is almost unchanged due to the polymer adsorption at the interface, there is no need of any external constraints to force the polymer chain to stay at the interface, and standard equilibrium MD simulations can be performed. All simulations were performed using the GROMACS simulation package version 4.5.4²¹ in the NPT ensemble with reduced temperature and pressure of $T^* = 1$ and $P^* = 1$, respectively. More details of simulations can be found in the [Supporting Information](#).

When polymers adsorb onto interfaces, they often adopt a pancake-like conformation. This can be seen from the eigenvalues of their gyration tensor in the plane of the interface (xy), $R_{g\parallel}$, with $R_{g\parallel} = (R_{gx}^2 + R_{gy}^2)^{1/2}$, against the number of monomers, N , in [Figure 1](#). The scaling law obtained is $R_{g\parallel} \sim N^{\nu}$, with $\nu = 0.74$, in agreement with the analytical exponent predicted for a two-dimensional random walk $\nu = 0.75$.¹⁷ This result shows that, although there are no constraints imposed in the model, the polymer chain sticks at the interface during the whole simulation and structurally behaves as if it is confined in a rigid 2D slit or strongly adsorbed on a solid surface. The same exponent can be obtained if, instead of using $R_{g\parallel}$, the 3D R_g value were used. The z (perpendicular to the surface) component of the radius of gyration is indeed constant and equal to σ , indicating that the confinement of the polymer is commensurable with the monomer size. [Figure 1](#) also reports the results obtained from simulations performed in bulk solution for which the same scaling law but with the expected Flory exponent of $\nu = 0.60$ was obtained.²²

The dynamical properties of the polymer have been studied in terms of end-to-end relaxation time (τ_R), central monomer (g_1), and polymer center of mass (g_3) mean square displacement

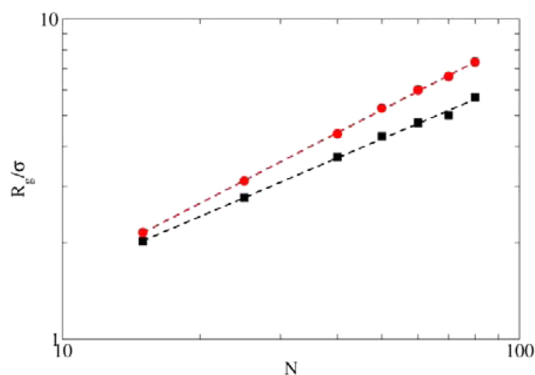


Figure 1. Radius of gyration (xy component only for the interface simulations (errors calculated as the standard deviation of the mean are less than $10^{-3}\sigma$) against number of monomer in the chain: red circles, interfacial simulation data; black squares, bulk simulations. The dotted lines represent the best fitting of the data points.

$$g_i(t) = \langle [R_i(t) - R_i(0)]^2 \rangle \quad (1)$$

where $R_i(t)$ represents the position of the central monomer (R_1) or polymer center of mass (R_3) at time t .

The corresponding diffusion time (τ_{diff}) is defined as the time required for a chain to move a distance of the order of its size

$$g_1(\tau_{\text{diff}}^1) = g_3(\tau_{\text{diff}}^3) = g_3(\tau_{\text{diff}}) = R_g^2 \quad (2)$$

where $\tau_{\text{diff}}^1 = \tau_{\text{diff}}^3 = \tau_{\text{diff}}$.

We have considered primarily these parameters since it has been shown that the diffusion coefficient, D

$$2dD = \lim_{t \rightarrow \infty} \frac{\langle [R_3(t) - R_3(0)]^2 \rangle}{t} \quad (3)$$

where d corresponds to the dimension of the confinement ($d = 2$ for the polymer at the interface and $d = 3$ in bulk solvent) depends on the simulation box size, L .²³ This dependence due to the long-range hydrodynamic effect is almost not observable in other dynamical properties such as τ_R .²⁴ The value of the end-to-end distance relaxation time, τ_R , can be obtained fitting the autocorrelation function, $C(t)$, of the end-to-end distance, R , to an exponential function

$$C(t) = C_0 \exp(-t/\tau_R) \quad (4)$$

the fitting is performed until $C(t)$ becomes negative. [Figure 2](#) reports the value of τ_R (the values are reported along with their errors in [Table 1S](#), in the [Supporting Information](#)) plotted against the number of monomers, N . The values obtained from the simulations performed in bulk solvent show the expected scaling law for a polymer in solution with HI, $\tau_R \sim N^{3\nu}$, known as Zimm model, where ν is the Flory exponent and is equal to $\nu = 0.588$ in good solvent (0.60 ± 0.2 from our simulations, see [Figure 1](#)). The fitting exponent obtained from the simulation (1.79 ± 0.19) is in good agreement with the theory (1.77) and previous simulations.^{22–24} The data obtained from the simulation with the interface can be fitted with the same scaling law, but the exponent is this time 2.05 ± 0.23 , in good agreement with the value typical of the Zimm model (2.19) and smaller than that expected if the polymer followed either the Rouse model (2.54) or the reptation, where $\tau_R \sim N^3$ (in the latter case, the exponent is independent from the value of the Flory parameter, ν). In order to establish internal consistency in our results, we plot the values of τ_R against the R_g values ($R_{g\parallel}$

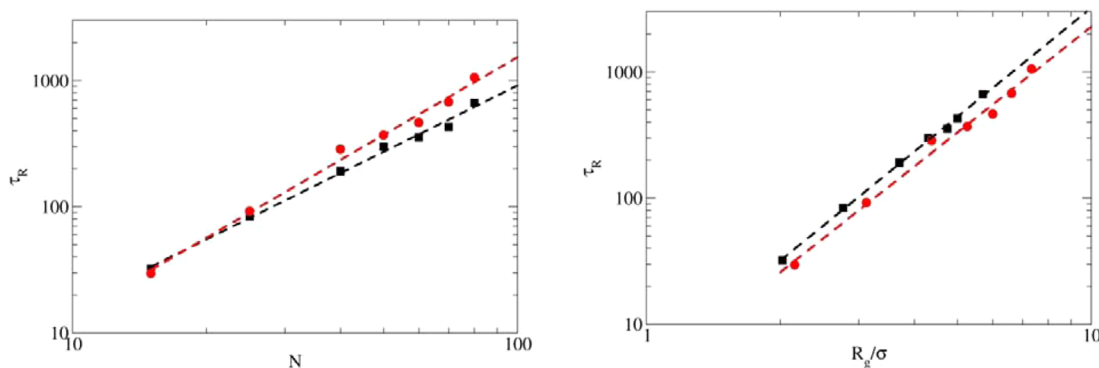


Figure 2. Logarithmic plot of the relaxation time, τ_R (in unit of τ), calculated from the autocorrelation time of the end-to-end distance (errors are smaller than the symbols size and reported in Table 1S) as a function of the chain length, N , and radius of gyration, R_g . Dashed lines indicate the best fitting for the data. Symbols as in Figure 1.

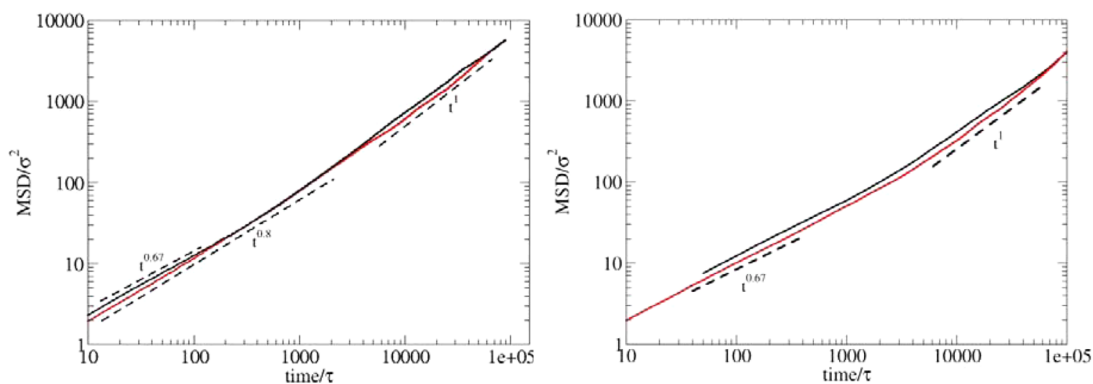


Figure 3. Time-dependence of mean-square displacement (MSD) of the central monomer, g_1 , for $N = 25$ (left) and 60 (right). The solid black line represents the data obtained in bulk solution, while the solid red line represents the results of the interfacial simulations. The dashed lines indicate the different slopes.

for the interfacial simulations). Using the scaling law theory, the values can be again fitted with a power function: the Zimm model predicts that $\tau_R \sim R_g^3$, while the Rouse model predicts that $\tau_R \sim R_g^{2+1/\nu}$. The exponent obtained from our simulation data is 2.8 ± 0.30 for both the bulk and interface model in agreement with the Zimm model and far off from the Rouse exponents (3.7 for bulk solution and 3.3 for 2D confinement).

The Zimm-like dynamics can also be seen from the central monomer mean square displacement (g_1 ; see eq 1) obtained for the confined and bulk polymeric systems and noticed that a crossover between two different dynamical behaviors occurs for $N = 40$. Figure 3 shows g_1 calculated for two polymer chains with a molecular weight below and above $N = 40$ ($N = 25$ and 60). The plots reveal that the subdiffusive behavior shown by short chains at the interface deviates from that typical of the Zimm model. Polymer dynamic theory predicts²² three dynamical regimes for polymer in solution: at short times ($t < \tau_m$), g_1 should be proportional to the time ($g_1 \sim t$); for intermediate times ($\tau_m < t < \tau$), $g_1 \sim t^\gamma$ with $\gamma = 0.67$ for the Zimm model and $\gamma = 0.54$ if the chain dynamics obeys the Rouse model; for long times ($t > \tau_m$), g_1 shows the final diffusive regime and becomes proportional to t . Here, long chains, $N > 40$, show indeed the Zimm exponent in their subdiffusive regimes, although a fourth regime with $g_1 \sim t^{0.8}$ can also be observed in both bulk solvent and interfacial simulations. This fourth regime has also been observed by Azuma and Takayama²⁵ for self-avoiding polymer confined in a pore slit with regularly distributed obstacles and more recently

by Desai et al.¹⁴ However, what is more interesting is that, for chains shorter than 40 monomers, the subdiffusive regime does not follow either the theoretical Zimm exponent or the Rouse one, but presents a much higher value equal to $\gamma = 0.8$. Figure 4

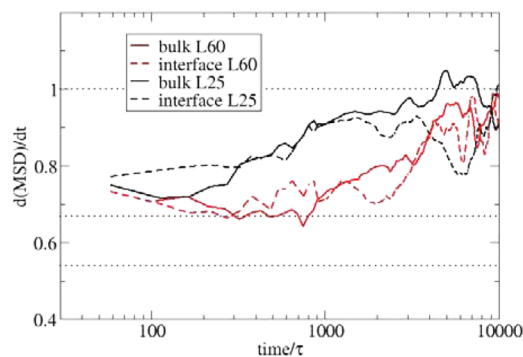


Figure 4. Slope of the mean-squared displacement (MSD) as a function of time. The horizontal pointed lines indicate slope equal 1, 0.67, and 0.54 from the top to the bottom.

shows the time evolution of the subdiffusive exponents for short polymer chains ($N = 25$) and long ones ($N = 60$; results for $N = 15$ and 50 for comparison are reported in the Supporting Information, Figure S1). It can be observed that, in bulk solution, short polymer chains already present a value of γ that is higher (around 0.70) than the expected Zimm value. In bulk solution this behavior has already been observed^{23,24} and it

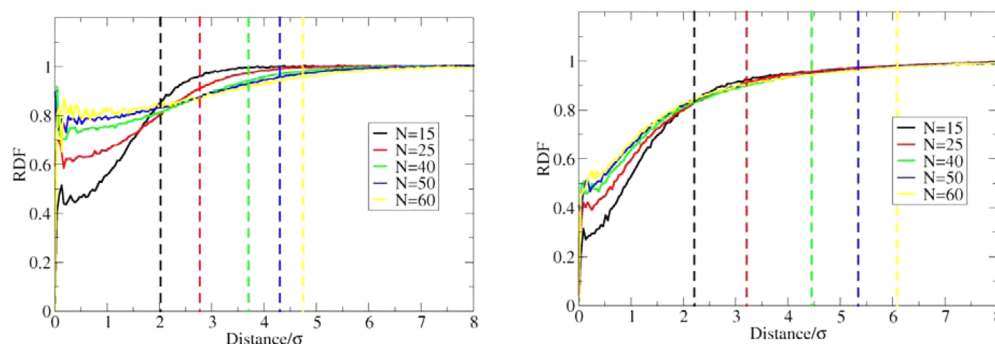


Figure 5. Radial distribution function (RDF) calculated between the center of mass of the polymer and the solvent beads for chains of different lengths: (left) the polymer is in bulk; (right) the polymer is at the interface. The dashed lines indicate the radius of gyration for the various polymer chains.

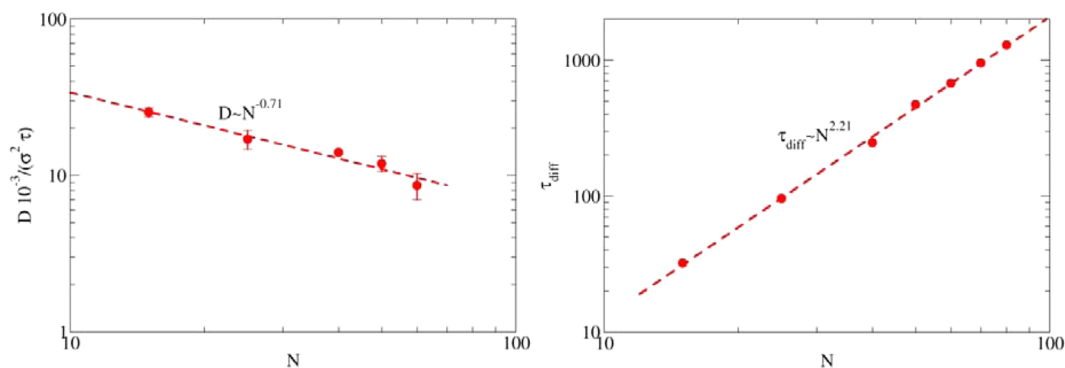


Figure 6. Plot of the values of diffusion coefficient, D , for the central monomer and the relaxation time of its diffusive motion, τ_{diff} against the chain length, N . The dashed lines indicate the best fitting of the data.

has been ascribed to the increasing effect that the end-monomer dynamics has on the central monomer ones for low molecular weight polymers.²⁴ The absence of a clear subdiffusive Zimm regime for short polymer chains becomes more evident when they are confined at the interface (Figure 4). Moreover, it seems that short chains remain trapped in a semidiffusive regime and take a longer time to reach Fickian diffusion compared with when they are immersed in the fluid. This again illustrates that the difference between interfacial and bulk dynamics depends on the polymer size; for larger molecular weights ($N > 40$), the chain relaxation (measured via its τ_R) is slower in bulk than at the interface, whereas for shorter polymer chains, the τ_R calculated in bulk and at interface is almost identical. This behavior is probably related to the fact that short polymer chains do not assume the coil-like structure typical of high molecular weight polymers, but instead, they maintain a fairly elongated conformation in solution of good solvent (see also the R_g values in Figure 1). This elongated shape might justify also the high subdiffusive exponent γ observed for short polymers in bulk. Indeed, the presence of a subdiffusive regime arises from the fact that when the polymer moves it must drag some of the solvent particles with it. For coil-like structure polymer, the solvent particles permeate inside the coil, while for short polymer chains, the number of solvent molecules near the center of mass of the polymer is smaller (see Figure 5); therefore, fewer solvent particles are bound to the chain and it experiences less drag. To investigate the dynamics of the solvent beads, the averaged residence time (t) of a solvent bead within a distance d , with $d = r_c = 2.5\sigma$, is calculated; t is obtained from the numerical integration of the autocorrelation function $C(t) = \langle \sum h(t_0)h(t_0 + t) \rangle / \langle \sum h(t_0)^2 \rangle$, where $h(t)$ is a step function equal to 1 if the solvent bead is within a distance d from a polymer bead at time t and otherwise set to zero. The autocorrelation functions calculated for L25 and L50 both in bulk solvent and at the interface and the values of t are reported, respectively, in Figure 1S and Table 2S of the Supporting Information. The results show that the solvent beads at the interface move faster than those in bulk, however, their dynamics is the same, irrespective of the polymer molecular weight.

Further confirmation of the Zimm-like dynamics comes from considering the diffusion coefficient, D , and the relaxation time of the central monomer diffusive motion, τ_{diff} . Shown in Figure 6 are D and τ_{diff} for polymers at the interface. Again, the simulations give results that are in closer agreement to the Zimm model, where $D \sim N^{-\nu}$ and $\tau_{\text{diff}} \sim N^{(2\nu+1)}$ than the Rouse or reptation models. These data are reported for polymer chains up to $N = 60$. As for longer chains, the error in D remains significant even after 10^8 simulation time-steps. The Zimm-like behavior for free-standing soft membrane was recently predicted by means of Brownian dynamics theory.²⁰ Analytically deriving the mobility tensor, the authors predicted a crossover between Zimm-like to a Rouse-like regime moving from a free-standing membrane to one confined between two solid walls. To test this prediction, the MSDs calculated from simulations where the liquid/liquid interface is sandwiched between two solid (attractive) walls (see Figure 4S in the Supporting Information) are compared with that obtained for a free-standing interface. The comparison is limited to L25. The computational results show that when the distance between the walls is larger than 4σ , the polymer dynamics still follows the Zimm-like model. But when the distance between the walls

is smaller than 4σ , the polymer dynamics deviates from the Zimm-like model and follows a Rouse-like regime. This crossover is observed for all the polymer chains considered here, and it is in agreement with the predictions of the Brownian dynamics theory.²⁰

reaches 4σ , the interface between the two liquids becomes unstable and breaks. Since the polymer still tends to lower the liquid/liquid interfacial area, the chain bends and part adsorbs on the newly formed liquid/liquid interface and part adsorbs on the walls (see Figure 4S in the Supporting Information). When such a transition occurs, the Rouse dynamics is recovered (see Figure 3S).

In conclusion, through molecular simulations we have demonstrated that both polymer structure and dynamics can change upon adsorption at a liquid–liquid interface. While the structure undergoes a change to a “pancake” conformation similar to that observed for polymers adsorbed on solid–liquid interfaces, the dynamical properties do not obey the Rouse or reptation behavior observed on solid surfaces. Rather, the hydrodynamic interactions, which in the latter case appear to be screened by the presence of the surface, still dominate, and the polymer dynamics is described by the Zimm-law as for a polymer in dilute solution. The effect that the presence of the interface has on the polymer dynamics can be appreciated only in the subdiffusive regime which, for short polymer chains, almost disappears. We ascribe this reduced drag effect of the solvent beads to their low density at the interface. These results indicate that the damping of the hydrodynamics interactions experimentally observed for polymer adsorbed on lipid bilayers is probably not due to the softness of the interface. Our simulation results are in agreement with recent theoretical results²⁰ which indeed indicate that a Zimm-like behavior is expected for polymer adsorbed on free-standing membrane and observed Rouse-like dynamics only for membranes under high confinement.

■ ASSOCIATED CONTENT

📄 Supporting Information

The Supporting Information is available free of charge on the ACS Publications website at DOI: 10.1021/acsmacrolett.5b00462.

Simulation details, table with the relaxation and residence times, and plots of the autocorrelation function, $C(t)$, slope of the mean-squared displacement as a function of time, and snapshots of the system sandwiched between two walls (PDF).

■ AUTHOR INFORMATION

Corresponding Author

*E-mail: paola.carbone@manchester.ac.uk.

Notes

The authors declare no competing financial interest.

■ ACKNOWLEDGMENTS

The authors acknowledge the assistance given by IT Services and the use of the Computational Shared Facility at The University of Manchester.

■ REFERENCES

- (1) Bae, S. C.; Granick, S. *Annu. Rev. Phys. Chem.* **2007**, *58*, 353–374.
- (2) Di Pasquale, N.; Marchisio, D. L.; Barresi, A. A.; Carbone, P. *J. Phys. Chem. B* **2014**, *118* (46), 13258–13267.
- (3) Nawaz, S.; Redhead, M.; Mantovani, G.; Alexander, C.; Bosquillon, C.; Carbone, P. *Soft Matter* **2012**, *8*, 6744–6754.
- (4) Taddese, T.; Carbone, P.; Cheung, D. L. *Soft Matter* **2015**, *11*, 81–93.
- (5) Cheung, D. L.; Carbone, P. *Soft Matter* **2013**, *9*, 6841–6850.

- (6) Halperin, A.; Pincus, P. *Macromolecules* **1986**, *19*, 79–84.
- (7) Nawaz, S.; Carbone, P. *J. Phys. Chem. B* **2011**, *115*, 12019–12027.
- (8) Xie, A. F.; Granick, S. *Nat. Mater.* **2002**, *1*, 129–133.
- (9) Zhang, L.; Granick, S. *Proc. Natl. Acad. Sci. U. S. A.* **2005**, *102*, 9118–9121.
- (10) Maier, B.; Rädler, J. O. *Phys. Rev. Lett.* **1999**, *82*, 1911–1914.
- (11) Desai, T. G.; Keblinski, P.; Kumar, S. K.; Granick, S. *Phys. Rev. Lett.* **2007**, *98*, 218301.
- (12) Qian, H.-J.; Chen, L.-J.; Lu, Z.-Y.; Li, Z.-S. *Phys. Rev. Lett.* **2007**, *99*, 068301.
- (13) Andrey, M. *J. Phys.: Condens. Matter* **2011**, *23*, 103101.
- (14) Desai, T. G.; Keblinski, P.; Kumar, S. K.; Granick, S. *J. Chem. Phys.* **2006**, *124*, 084904.
- (15) Descas, R.; Sommer, J.-U.; Blumen, A. *J. Chem. Phys.* **2005**, *122*, 134903.
- (16) Dimitrov, D. I.; Milchev, A.; Binder, K.; Klushin, L. I.; Skvortsov, A. M. *J. Chem. Phys.* **2008**, *128*, 234902.
- (17) Milchev, A.; Binder, K. *Macromolecules* **1996**, *29*, 343–354.
- (18) Patra, T. K.; Singh, J. K. *J. Chem. Phys.* **2014**, *140*, 204909.
- (19) Mukherji, D.; Bartels, G.; Müser, M. H. *Phys. Rev. Lett.* **2008**, *100*, 068301.
- (20) Ramachandran, S.; Komura, S.; Seki, K.; Gompper, G. *Eur. Phys. J. E: Soft Matter Biol. Phys.* **2011**, *34*, 46.
- (21) Hess, B.; Kutzner, C.; van der Spoel, D.; Lindahl, E. *J. Chem. Theory Comput.* **2008**, *4*, 435–447.
- (22) Rubinstein, M.; Colby, R. H. *Polymer Physics*; Oxford University Press: New York, 2003.
- (23) Dünweg, B.; Kremer, K. *J. Chem. Phys.* **1993**, *99*, 6983–6997.
- (24) Jiang, W.; Huang, J.; Wang, Y.; Laradji, M. *J. Chem. Phys.* **2007**, *126*, 044901.
- (25) Azuma, R.; Takayama, H. *J. Chem. Phys.* **1999**, *111*, 8666–8671.